NMR STUDY OF FLUORIDE ION DIFFUSION IN POTASSIUM-DOPED β-PbF_2

Thesis by

David M. Cannon

In Partial Fulfillment of the Requirements

for the Degree of

Master of Science

California Institute of Technology

Pasadena, California

1978

(Submitted March 10, 1978)

ACKNOWLEDGMENTS

I wish to thank the California Institute of Technology and the A.R.C.S. Foundation for their financial support. I am very grateful to Professor Robert Vaughan for his patient assistance in scientific matters as well as for his friendship and concern toward me as an individual. It has been a real pleasure to associate with the other members of the Vaughan group, both in and out of the lab. Finally, greatest thanks are extended to my wife Ana Maria. I cannot adequately express my appreciation for her patience, selflessness, and encouragement. This thesis is dedicated to her.

ABSTRACT

Fluoride ion motion in a KF-doped β-PbF_2 crystal was studied by measuring the ^{19}F relaxation times T_1, T_2, and $T_{1\rho}$. Measurements were made on a 56.4 MHz pulsed spectrometer over the temperature range -101°C to 22°C; the $T_{1\rho}$ data were taken in a rotating magnetic field of 6.8 G. Two sets of T_2 data were taken, yielding activation energies of 0.17 ± 0.01 eV and 0.18 ± 0.01 eV. Activation energies obtained from T_1 and $T_{1\rho}$ data were 0.17 ± 0.01 eV and 0.34 ± 0.02 eV, and a correlation time of 2.9 μsec was observed at -20°C, the temperature at which the $T_{1\rho}$ minimum occurs. Comparison of these data with previously published results shows that potassium-doping is more effective than sodium-doping in activating fluorine motion. It is believed that T_1 relaxation is dominated by a mechanism other than anionic diffusion.

TABLE OF CONTENTS

I. NMR RELAXATION PROCESSES AND SOLID STATE DIFFUSION

The experimental work described in this thesis involves the use of NMR techniques to study anion diffusion in the fast ionic conductor β-PbF_2. Specifically, the relaxation times T_1, T_2, and $T_{1\rho}$ were measured as a function of temperature. Accordingly, this section gives a brief discussion of these relaxation processes and their relationship to solid state diffusion.

If a sample containing a non-zero nuclear magnetic moment is placed in a magnetic field, a small component of magnetization will form in the z direction (along the field). This magnetization can be rotated to the xy plane by a radio-frequency (rf) pulse with effective field perpendicular to the z direction. After the pulse, the component of magnetization in the xy plane (M_{xy}) will begin to shrink. For a liquid or motionally narrowed solid, M_{xy} will be seen to decay exponentially with a time constant T_2, the spin-spin relaxation time. Simultaneously the z component of magnetization will return exponentially to its equilibrium value; the time constant for this process is called T_1.

The width of an NMR line in frequency space contains contributions from several sources. There is a contribution from $1/T_1$ due to the finite lifetime of a nucleus in any eigenstate. Magnetic field inhomogeneities may also broaden a line. For solids, however, the largest contribution to the linewidth usually comes from dipole-dipole interactions between nuclei.

T_1 processes involve energy exchange between the nuclear spins and the lattice. Following any process which destroys the thermal

equilibrium between spins and lattice, T_1 processes restore the two systems to equilibrium. Consequently, T_1 is known as the spin-lattice relaxation time.

A third relaxation process is called $T_{1\rho}$, or T_1 in the rotating frame. In a $T_{1\rho}$ experiment, an rf pulse along the x' axis rotates the magnetization until it lies along the y' axis (x' and y' are axes in a reference frame which rotates about the z axis at the radio frequency). Immediately after the pulse, the phase of the rf signal is changed by 90° and a "locking" field along the y' axis is generated. The magnetization then relaxes along the y' axis in a process similar to T_1. The major difference is that the locking field in a $T_{1\rho}$ experiment is several orders of magnitude smaller than the Zeeman field along which T_1 relaxation takes place. This makes $T_{1\rho}$ more sensitive to low frequency motions than T_1.

T_2, T_1, and $T_{1\rho}$ relaxation processes are induced by microscopic fluctuations in the magnetic field at individual nuclei. Such fluctuations can be caused by the bodily movement of nuclear dipoles through the lattice, a situation which occurs when diffusion takes place. The direction and frequency of these fluctuations are important. They must occur in a direction perpendicular to the direction of relaxation and are most effective if they have the same frequency as the rotating magnetization. From these considerations several qualitative predictions can be made. T_1 relaxation should be most effectively induced by fluctuations in the xy plane at the Larmor frequency $\omega_o = \gamma H_o$ (γ is the gyromagnetic ratio of the nuclei and H_o is the strength of the static Zeeman field). Similarly T_2 processes

should be effected by xy fluctuations at ω_o and also by static and very low frequency ($\omega \approx 0$) movements in the z direction. We expect $T_{1\rho}$ to be caused by frequencies at ω_o as well as by those near $\omega_1 = \gamma H_1$ where H_1 is the strength of the locking field.

These statements can be more quantitatively expressed by the use of a "correlation function" $G(\tau)$ and its Fourier transform the "spectral density function" $J(\omega)$. One may think of $G(\tau)$ as the probability that a nucleus will experience the same magnetic environment at time t as it did at time $t' = t-\tau$. The correlation function is characterized by some critical time τ_c, called the "correlation time." For diffusing nuclei, τ_c is the average time between hops. Taking the Fourier transform of $G(\tau)$ gives $J(\omega)$, a function which gives the motional frequencies of hopping nuclei. It contains frequencies up to approximately $\omega = 1/\tau_c$. The relaxation rates $1/T_1$, $1/T_2$, and $1/T_{1\rho}$ are simply linear combinations of spectral density functions.

An important property of the spectral density function is that the area under the curve, i.e., $\int_{-\infty}^{+\infty} J(\omega)d\omega$, does not vary with τ_c. If $J(\omega)$ is plotted for several values of τ_c, it is seen in Fig. 1 that for a specific value of $\omega = \omega'$, $J(\omega')$ has a maximum value for $\tau_c = 1/\omega'$. Since for T_1, we are interested in Fourier components at $\omega = \omega_o$, we expect that a plot of T_1 vs. τ_c will have a minimum when $\tau_c = 1/\omega_o$. Similarly, $T_{1\rho}$ vs. τ_c should have a minimum near $\tau_c = 1/\omega_1$.

Using the functions $G(\tau)$ and $J(\omega)$, various quantitative expressions have been derived for relaxation rates in terms of spectral density functions. For dipole-dipole interactions

between identical spins, the following have been obtained.[1,2]

$$1/T_1 = C\{J(\omega_o) + 4J(2\omega_o)\} \tag{1}$$

$$1/T_2 = C\{\tfrac{3}{2}J(0) + \tfrac{5}{2}J(\omega_o) + J(2\omega_o)\} \tag{2}$$

$$1/T_{1\rho} = C\{\tfrac{3}{2}J(2\omega_1) + \tfrac{5}{2}J(\omega_o) + J(2\omega_o)\} \tag{3}$$

Here C is a constant for a given material.

In order to evaluate these expressions, the functions $J(\omega)$ must be known. Normally an exponential correlation function is assumed:

$$G(\tau) = h^2\exp\{-|\tau|/\tau_c\} \tag{4}$$

where h^2 is a measure of the strength of interaction between nuclei. It then follows that the spectral density function is a Lorentzian:

$$J(\omega) = 2h^2\tau_c/\{1 + (\omega\tau_c)^2\}. \tag{5}$$

Combining (5) with (1), (2), and (3) gives expressions for T_1, T_2, and $T_{1\rho}$ in terms of τ_c. Fig. 2 gives a typical plot of ln (T_1, T_2, and $T_{1\rho}$) vs. ln τ_c. The curve for T_2 has been drawn to reflect the fact that for very long τ_c, T_2 assumes a rigid lattice value. As τ_c becomes shorter, T_2 begins to increase, resulting in motional narrowing of the resonance line. T_1 has a minimum when $\tau_c = 1/2\omega_o$ whereas $T_{1\rho}$ reaches its minimum at $\tau_c = 1/2\omega_1$. Since $\omega_o >> \omega_1$,

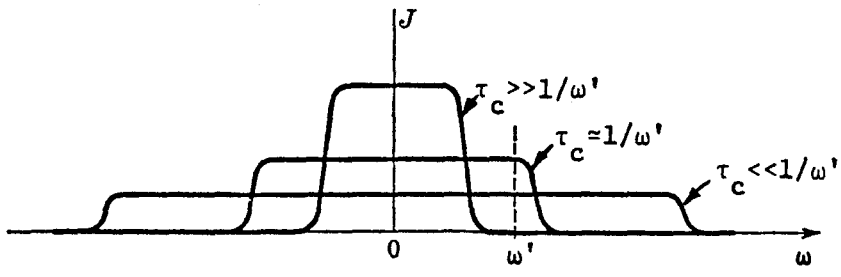

Fig. 1. $J(\omega)$ plotted for three values of τ_c. $J(\omega')$ has its maximum value for $\tau_c = 1/\omega'$.

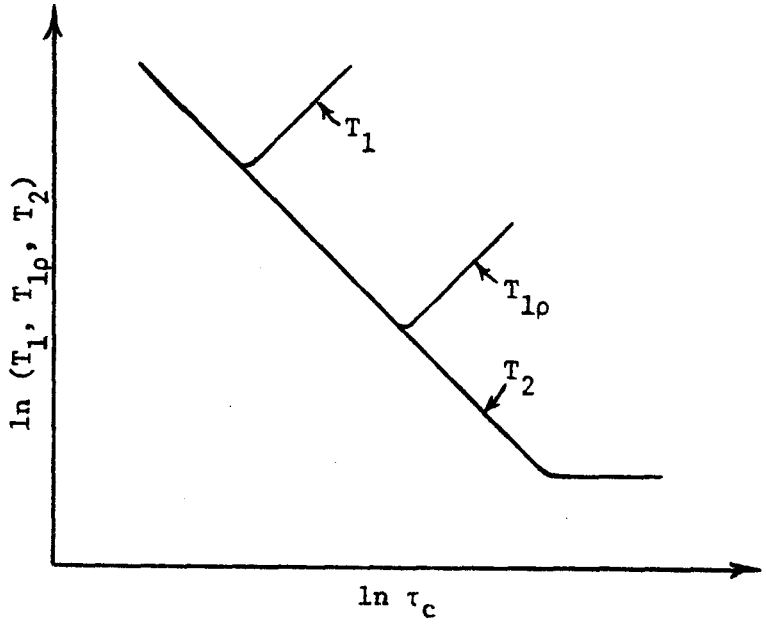

Fig. 2. Typical relaxation curves ln (T_1, $T_{1\rho}$, T_2) vs. ln τ_c.

$T_{1\rho}$ is more sensitive to low frequency motions than is T_1. To the left and right of the minima the plots of ln T_1 and ln $T_{1\rho}$ are linear with slopes of -1 and +1. For short τ_c ($\tau_c << 1/\omega_o$) the three relaxation rates become equal.

How does the measurement of NMR relaxation rates contribute to an understanding of solid state diffusion? The answer to this lies in the fact that correlation times are an essential feature of both processes, relaxation and diffusion. For simple diffusion, the diffusion coefficient $D \propto \Gamma$, where $\Gamma = 1/\tau_c$ is the jump frequency. Furthermore, for thermally activated motion with an activation energy E*, the jump frequency is given by

$$\Gamma = \Gamma_\infty \exp(-E^*/kT). \tag{6}$$

When this situation occurs

$$\ln \tau_c = -\ln \Gamma_\infty + E^*/kT \tag{7}$$

and a plot of ln (T_1, T_2, $T_{1\rho}$) vs. 1/T will have the form given in Fig. 2. The slope of the lines gives a value for E*, and the value of τ_c can be determined for the temperatures at which T_1 and $T_{1\rho}$ minima occur.

This approach to studying solid state diffusion nicely complements more traditional methods which directly measure bulk diffusion properties. The latter techniques can be used only indirectly to infer atomic mechanisms which cause diffusion. In contrast, the

NMR approach does not directly measure diffusion but is a more straightforward means of determining atomic behavior. The combined use of these two approaches can be valuable in elucidating the atomic mechanisms which effect diffusion.

References

[1] A. Abragam, The Principles of Nuclear Magnetism (Oxford University Press, London, 1961), ch. 8.

[2] J.B. Boyce, J.C. Mikkelsen, and M. O'Keeffe, Solid State Commun. 21, 955 (1977).

may be attainable. Accordingly, some effort has been made to ascertain the mechanism of ionic motion in PbF_2, but no unequivocal model has as yet emerged. This introduction gives a brief survey of the work which has been done to characterize ionic diffusion in this substance.

Lead fluoride is known to occur in two crystal structures. The orthorhombic α form is generally considered the low-temperature form. Upon heating, this is changed to the cubic β form, which has the CaF_2 (fluorite) structure (see Fig. 3).[1] Sauka[2] reported that this structure change occurs at 315°C, whereas Kennedy et al.[3] observed the transition in the range 334°-344°; others have reported temperatures of 200°-400°C.[2] After cooling, the β structure may be retained metastably; its melting point is recorded as 822°C.[4] Of the two structures, the β modification is the better ionic conductor, and most research has involved that form. Hereafter, all references to PbF_2 in this thesis will designate the β form unless explicitly stated otherwise.

Most studies of ionic motion in β-PbF_2 have involved conductivity measurements. In 1921, Tubandt[5] measured the transport numbers of the lead and fluoride ions and reported that only fluoride ion motion contributed to the conductivity. More recently, Kennedy et al.[3] measured a negative ion transference number of 0.93 for pure β-PbF_2, and Liang and Joshi[6] observed a similar value of 0.94 for α-PbF_2 doped with YF_3. Additional studies[3, 7-9] have been made to determine the electronic contribution to the total conductivity; these have produced values in the range 10^{-4}-1.0% for the electronic contribution under various conditions. Taken together, these results demonstrate that the conducting properties of PbF_2 are a result of ionic motion

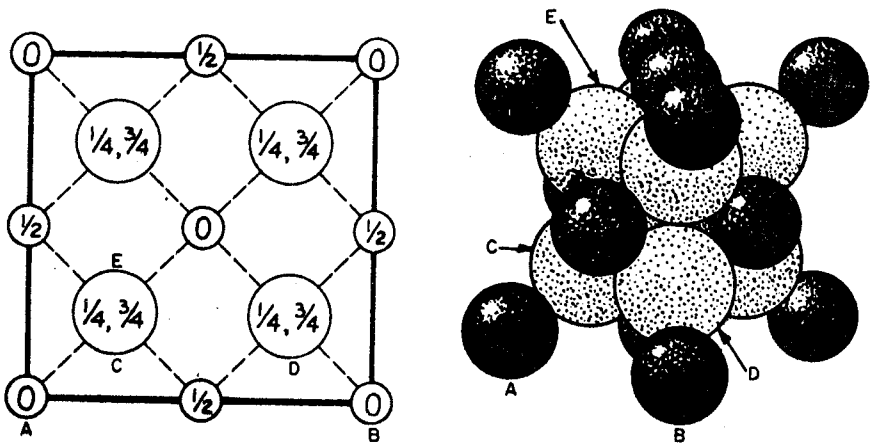

Fig. 3a (left). The positions of the atoms within the unit cell of fluorite, CaF_2, projected on a cube face. Lettered circles refer to the corresponding spheres of Fig. 3b.

Fig. 3b (right). A perspective packing drawing showing the distribution of the atoms of CaF_2 within the unit cube.

within the fluoride sublattice.

This conductivity is thermally activated, and a number of investigations[3,6-19] have been made concerning the temperature dependence of the conductivity. These have led to the recognition of three roughly defined sections in the σ vs. T curve for nominally pure lead fluoride. These sections are distinguished by differing values of ΔH, the activation enthalpy, in the three temperature regions.

The room-temperature conductivity of pure β-PbF_2 is near 10^{-8} $(ohm\text{-}cm)^{-1}$. As the temperature is raised, the conductivity increases with an activation energy which has generally been reported in the range 0.50-0.70 eV. Several studies[10,15,16,18] have indicated that at some elevated temperature, σ begins to increase more rapidly (ΔH increases), indicating the possibility that a different diffusion mechanism prevails in this second temperature region. This change in behavior has been observed at temperatures in the range 180°-310°C. However, other investigators have gone to even higher temperatures without observing an increase in ΔH. This is indicative of the lack of agreement which exists in conductivity data for "pure" PbF_2. A summary of such data is presented in Table 1.

A third type of conductivity behavior is observed at very high temperature. Derrington and O'Keeffe[19] observed a sharp decrease in ΔH from 450°-575°C: σ remained almost constant as the temperature was increased from 575°C through the melting point. Benz[7] noted a similar decrease in ΔH near 400°C. Both studies published a conductivity of ~ 1 $(ohm\text{-}cm)^{-1}$ at the inflection point. This high temperature

Table 1. Summary of conductivity studies of nominally pure β-PbF_2.

Authors	Crystal	Temp. Range (°C)	ΔH (eV)	-log σ at 25°C $(ohm\text{-}cm)^{-1}$
Kennedy et al.[3]	poly	25-250	.47-.51	---
	single	25-250	.60-.65	7.7
Schoonman et al.[10]	single	25-200	.70	7.9
		200-400	.94[a]	---
Gianduzzo et al.[11]	poly	25-150	.47	7.1-8.0
Liang and Joshi[6]	poly	25-350	.62	7.1
Reau et al.[12]	---	30-200	.45	---
Arkhangel'skaya et al.[13]	single	-50-25	.8	6.3
Schoonman et al.[14]	poly	25-350	.68	7.2
Kennedy and Miles[15]	poly	25-180	.39-.50	6.5
		180-310	.66	---
	single	25-150	.60	---
Bonne and Schoonman[16]	single	25-310	.66	7.8
		310-425	≈1	---
Raistrick et al.[17]	single	25-320	.63	7.5
Bonne and Schoonman[18]	poly, single	30-310	.67	7.8
		310-430	1.04	---

[a]The value was originally reported as 1.05 eV but was corrected in a later paper (see ref. 18).

behavior was interpreted[19] as being caused by a high degree of anion disorder, i.e., the anion sublattice had effectively melted even though the sample was still solid. This view was supported by the measurements of Derrington and O'Keeffe who observed virtually no change in the conductivity at the actual melting point of PbF_2. Their estimate indicated that at 727°C, more than one tenth of the anions were in motion at a given instant.

In order to better understand the mechanism of fluoride ion motion, several studies have been made using doped samples. The substitution of a monovalent metal ion in the PbF_2 lattice is expected to produce a fluoride ion vacancy. Similarly, the replacement of a PbF_2 unit with a trivalent impurity should create an interstitial anion. By using such impurity-doped samples, the effect of known defects upon the conductivity can be examined.

The results of conductivity experiments involving monovalent dopants are relatively unambiguous. Studies have been made on lead fluoride samples to which KF, NaF, and AgF dopants had been added.[6,15,18] See Table 2 for a summary of studies involving these doped samples. In each case, the effect of doping was to increase the conductivity and decrease the activation energy. Therefore, while there is some disagreement on details, it is well accepted that fluoride diffusion can be activated by anion vacancies.

The results for trivalent doping are less clear-cut (see Table 2). In an experiment using a BiF_3-doped sample, Kennedy and Miles[15] detected a decrease in conductivity and an increase in ΔH as compared to a nominally pure sample. Their interpretation was that diffusion

Table 2. Summary of conductivity studies of doped β-PbF_2. The upper part of the table cites studies involving monovalent dopants; the lower section gives data for trivalent-doped samples.

Authors	Crystal	Dopant	Temp. Range (°C)	ΔH (eV)	-log σ at 25°C $(ohm\text{-}cm)^{-1}$
Liang and Joshi[6]	poly	KF (.1-1 m/o)	25-300	.18	3.2-4.6
Kennedy and Miles[15]	poly	KF (.1-2 m/o)	25-180	.21-.33	3.1-4.6
		KF (.1 m/o)	180-280	.51	---
	poly	NaF (.5-1.5 m/o)	25-250	.22-.39	5.9 (.5 m/o)
Bonne and Schoonman[18]	single	AgF	30-130	.20	5.1
			130-290	∿.65	---
			290-430	∿1.0	---
Liang and Joshi[6]	poly	YF_3 (.3 m/o)	25-300	.62	6.8
Kennedy and Miles[15]	poly	BiF_3 (1 m/o)	25-225	.53	7.3
Joshi and Liang[9]	poly	AlF_3 (5-12 m/o)	-50-70	.36	4.0-5.0
	poly (annealed)	AlF_3 (5-12 m/o)	25-230	.52	5.2-5.7
			230-400	.30	---
Arkhangel'skaya et al.[13]	single	TmF_3, SmF_3, TbF_3, EuF_3, CrF_3 (.05-1.5 m/o)	-50-25	.8	5.2-6.0
Bonne and Schoonman[18]	single	LaF_3	30-330	.50	6.1
			330-430	∿1.0	---

proceeds only by a vacancy mechanism at low temperature. Other conductivity studies argue against this hypothesis. In an experiment involving trivalent rare-earth and Cr dopants, Arkhangel'skaya et al.[13] witnessed an increase in conductivity but observed no change in ΔH. Liang and Joshi[6] obtained a similar result for an YF_3-doped sample. They concluded that vacancies are responsible for diffusion in monovalent-doped samples, but that fluoride motion in pure and trivalent-doped samples is effected by an interstitial mechanism. They further suggested[20] that the anomalous results of Kennedy and Miles[15] may have been due to a reaction between BiF_3 and the Pb electrodes. An alternate explanation, however, is that the "pure" sample used by Kennedy and Miles contained a significant number of extrinsic vacancies, and that trivalent doping merely annihilated these defects. More recently, Bonne and Schoonman[18] found that σ increased and ΔH decreased upon addition of LaF_3 to lead fluoride samples. They ascribed this phenomenon to extrinsic interstitials but proposed that fluoride motion in pure PbF_2 occurs via a vacancy mechanism.

It thus appears that conductivity in β-PbF_2 can be increased by trivalent or by monovalent dopants. The effects of these impurities differ in degree, however, as seen in Table 2. Whereas doping with KF may increase the room temperature value of σ by three or four orders of magnitude, the substitution of trivalent dopants at comparable concentration levels produces a change of one or two orders of magnitude. It is also apparent that monovalent doping results in a significant decrease in activation energy, whereas the effect of trivalent impurities upon ΔH is much less obvious.

While it is apparent that the high conductivity of PbF_2 is due to

anion disorder, the exact nature of this disorder is not well understood. Most authors seem to agree that Frenkel disorder exists in the fluoride ion sublattice, and that diffusion may occur by either a vacancy or an interstitial mechanism. No consensus has been reached, however, concerning the relative contributions of these mechanisms to the total conductivity, nor whether diffusion in nominally pure β-PbF_2 is activated by extrinsic or intrinsic defects.

Although electrochemists have attempted to deal with these issues, there are several reasons why conclusions drawn from conductivity experiments alone may be tenuous.

1. In most cases, the purity of the samples in these studies was not known. If the conductivity is very sensitive to small impurity levels, deviations in reported data for "nominally pure" lead fluoride could be due to differences in sample composition.
2. The direct measurement of ionic conductivity requires the use of some form of electrode. This creates the possibility of interfacial effects which introduce uncertainty into any conclusions regarding bulk conductivity.
3. Even if interfacial effects could be entirely eliminated, a conductivity study would only demonstrate a macroscopic property of the material. Interpretation in terms of a microscopic model would be hazardous because there would be no way of separating effects due to such factors as grain boundary diffusion or sample inhomogeneity.

The use of NMR techniques to study anion motion in PbF_2 avoids

some of these problems. Obviously, the need for electrodes is eliminated. Since NMR looks at all the ^{19}F nuclei in a sample, it is possible to determine whether conductivity is due to motion of all the nuclei or to an effect such as grain boundary diffusion. The ^{19}F nucleus is easily detected and the movement of that ion through the lattice should be evidenced in the relaxation data as discussed in Chapter I of this thesis. If relaxation is dominated by a simple hopping motion of fluorine nuclei, curves similar to those depicted in Fig. 2 are expected. Deviations from that form would indicate a significant contribution from other relaxation mechanisms. Thus, by applying NMR techniques to the study of samples of well known composition, valuable information can be obtained regarding the nature of anion motion.

Although the application of NMR techniques to the lead fluoride problem has not been extensive, several studies[14, 21-26] have been made. These are summarized in Table 3.

The first NMR analysis was made by Mahajan and Rao[21] who measured the linewidth of α-PbF_2 over the temperature range -50°-190°C. They reported the onset of motional narrowing at -10°C and an activation energy of 0.35 eV. Comparison of these values with results obtained in later studies suggests that the sample used by Mahajan and Rao probably contained impurities which increased fluorine mobility.

Hwang, Engelsberg, and Lowe[23] did pulsed NMR measurements on PbF_2 in the cubic and orthorhombic forms and showed that ionic motion in the β structure was significantly greater than in the α. In the same paper, results were reported for a sample of β-PbF_2 which had been sodium-doped. It was found that this doping caused motional narrowing

Table 3. Summary of NMR studies of PbF_2.

Authors	Method	Crystal	Dopant	Onset of Mot. Nar. (°C)	ΔE (eV)
Mahajan and Rao[21]	cw, linewidth	poly α	---	-10	.35
Mahendroo et al.[22]	cw, linewidth	single β	---	50	---
		poly α	---	---	---
	pulsed, T_2	poly β	---	---	---
	pulsed, T_1		---	---	.32
Hwang et al.[23]	pulsed, T_2	single α	---	130	---
		single β	---	80	.73
		poly β	2 m/o NaF	-100	.32
Schoonman et al.[14]	cw, linewidth	poly β	.03-.09 m/o MnF_2	∿30	.59-.63
Hwang et al.[24]	pulsed, T_2	single β	0.12 m/o NaF	---	.27
	pulsed, T_1			---	.205
	pulsed, $T_{1\rho}$			---	.29
Boyce et al.[25]	pulsed, T_2	poly β	---	100	.74
	pulsed, T_1		---	---	.74
	pulsed, $T_{1\rho}$		---	---	.74

to occur at a much lower temperature (-100°C) than in the pure sample, and that the value of ΔE was significantly reduced. These findings agree qualitatively with results from conductivity experiments.

In order to more quantitatively compare results obtained by NMR and conductivity methods, Schoonman et al.[14] studied a polycrystalline sample of β-PbF_2 using each of the two approaches. They reported ΔH = .59-.63 eV from NMR linewidth measurements and ΔH = .68 eV from conductivity. Furthermore, they calculated the diffusion coefficient at 27°C from the two sets of data and obtained results which agreed to within a factor of 3.5. Their conclusion was that NMR line-narrowing and ionic conductivity were both caused by motion of all fluoride ions within the sample.

In a pulsed-NMR study of β-PbF_2, Hwang et al.[24] measured relaxation rates as a function of temperature for two Na-doped samples of well known chemical composition. It was found that $T_1 \propto 1/N$ and $T_2 \propto N$ where N is the ratio of doping levels in the two samples. Activation energies of 0.205, 0.27, and 0.29 eV were obtained for T_1, T_2, and $T_{1\rho}$ relaxation. Although T_2 showed a strong pressure dependence (as expected for a diffusional relaxation mechanism) T_1 was found to have little dependence upon pressure. Furthermore, the value for T_1 was found to be essentially independent of H_o even though data were taken in the long correlation-time region ($\tau_c >> 1/\omega_o$) where T_1 would be expected to be proportional to H_o^2 if T_1 were controlled by fluorine motion. These observations led Hwang et al. to conclude that fluoride ion diffusion was the controlling mechanism in T_2 and $T_{1\rho}$ relaxation, whereas T_1 was dominated by a different relaxation mechanism.

In addition to the NMR studies previously described, two experiments have been performed in which magnetic resonance was used to study PbF_2 at high temperature. Boyce, Mikkelsen, and O'Keeffe[25] measured T_1, T_2, and $T_{1\rho}$ to 700°C and observed anomalous changes in each of these parameters at 250°C and 450°C. Subsequently, Hogg, Vernon, and Jaccarino[26] measured the linewidth of a Mn-doped sample and found the same type of behavior at high temperatures. They speculated that these anomalies could be explained by the effects of paramagnetic impurity ions. These studies, however, are not directly relevant to the present work.

To summarize, it has been shown via conductivity and magnetic resonance experiments that substantial fluoride ion motion takes place in β-PbF_2. The degree to which this occurs is highly dependent upon impurities within the sample; the especially high sensitivity to monovalent dopants suggests that differences among various "pure" samples may be at least partially due to trace quantities of monovalent impurities. The alkaline earth fluorides, which have the same crystal structure as β-PbF_2, do not show this high degree of anion mobility, nor do they experience the same lowering of activation energy upon addition of monovalent dopants. The reasons for these differences are not known. Thus, a fundamental understanding of the diffusion mechanism in β-PbF_2 is still lacking.

The objective of the present experiment was to determine the effect of cation size upon fluorine mobility in monovalent-doped β-PbF_2. This was to be done by measuring T_1, T_2, and $T_{1\rho}$ as a function of temperature for a potassium-doped single crystal, and by comparing

these values with the data published by Hwang et al.[24] for a sodium-doped sample. Several interesting yet perplexing results have emerged from this work.

Experimental Details

A single crystal of potassium-doped (~0.01 wt %) was ordered from Optovac, Inc. Spectrographic and wet chemical analyses were made to determine chemical composition. These revealed the presence of 0.008 wt % potassium. The wet chemical analysis also detected sodium, but it is presently not known whether that is a real crystal impurity or a result of the analysis technique. At the time of this writing, an attempt is being made to obtain a mass spectrographic analysis of the sample.

An attempt was made to orient the crystal using the back-reflection Laue method. This was abandoned, however, when it was discovered that the crystal was severely twinned.

All NMR data were taken on a 56.4 MHz pulsed spectrometer. Temperature was varied between -101°C and 22°C, and temperature readings were generally accurate to ±2°C.

T_2 was obtained by recording the on-resonance free induction decay at each temperature. These fid's were interpreted as consisting of two components at temperatures above -60°C (see Results section). The T_2 values reported in this paper were obtained from the narrow-line component. This was done by plotting ln M_y vs. t and taking the slope of this curve for long t, after the signal from the broad-line component had become negligible.

T_1 was measured using a $90° - \tau - 90°$ pulse sequence (see Farrar and Becker,[27] pg. 22). This sequence was performed for at least five values of τ and a plot was made of ln $[A(\infty) - A(\tau)]$ vs. τ where $A(\infty)$ is the fid amplitude for $\tau \geq 5T_1$ and $A(\tau)$ is the fid amplitude for $\tau \sim T_1$.

These plots were nonlinear (see Results section), indicating the presence of more than one component. T_1 was taken as the slope of the line for short τ; this value for T_1 was believed to represent the spin-lattice relaxation time of the narrow-line component.

$T_{1\rho}$ was measured by producing a 90° pulse along the x' axis followed immediately by a holding pulse of length τ and amplitude 6.8 G along the y' axis. The amplitude, $A(\tau)$ of the fid obtained after termination of the holding pulse was recorded for at least five values of τ and a plot was made of $\ln A(\tau)$ vs. τ. $T_{1\rho}$ was taken as the slope of a line for short τ, corresponding to $T_{1\rho}$ of the narrow-line component.

Results

The crystal used in this study was of reasonably good quality as demonstrated by the clarity of its Laue photographs. Such a photograph is reproduced in Fig. 4. The crystal was not single, however, since different portions of the sample were found to have different orientations. It appeared that the crystal may have been composed of thin lammelae of alternating orientation.

Free induction decays were found to be Gaussian in the rigid-lattice temperature region. This is evidenced by the linearity of a plot of log M_y vs. t^2 for fid's in this regime (see Fig. 5).

As the temperature was raised, a motionally narrowed component began to appear at about -60°C. This component made an increasing contribution to the total signal as the temperature was further increased. At room temperature, ~96% of the signal came from the motionally narrowed component. Figs. 6 and 7 show fid's taken at two temperatures in this motionally narrowed regime. Decay of the narrow component is seen to be exponential.

T_1 and $T_{1\rho}$ decays were also seen to consist of more than one component as illustrated in Figs. 8 and 9. The values of T_1 and $T_{1\rho}$ for the narrow-line component were extracted by considering only the most rapidly decaying part of the curves.

Two different sets of T_2 data were obtained over the entire temperature range of interest. The first set of measurements, with values designated as $T_2(A)$, was made at the same time as the T_1 data were taken. Following these measurements was an interval of several weeks before the next data were taken. During that time it was decided

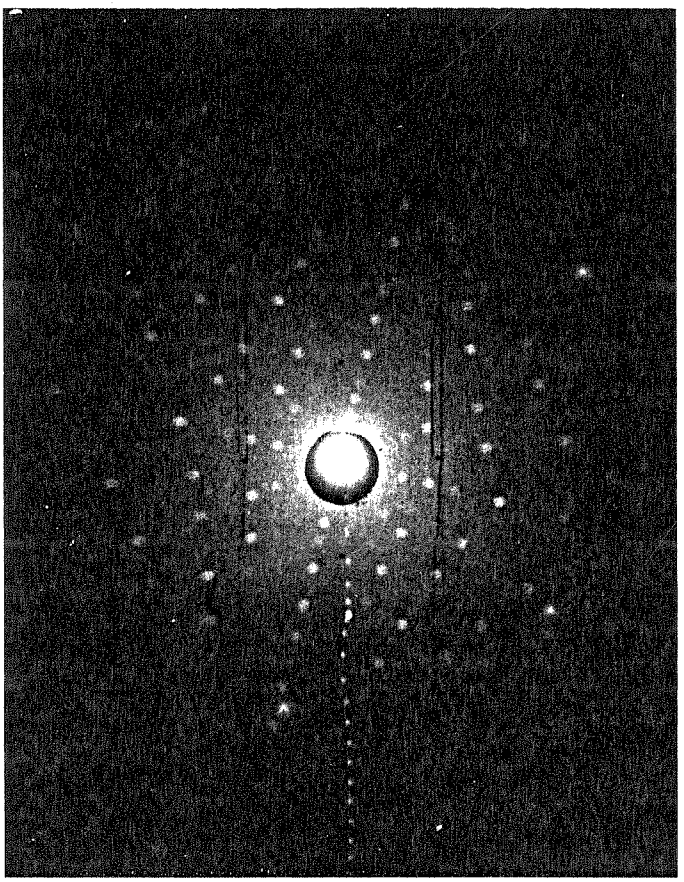

Fig. 4. Back-reflection Laue photograph of doped β-PbF_2 crystal. The portion of the crystal being examined is in the [110] orientation.

to repeat the T_2 experiment taking more signal averages. This was done concurrently with the $T_{1\rho}$ measurements, and values of T_2 obtained in this second set of measurements are denoted $T_2(B)$.

The values of T_2 obtained in these two data sets differ by a factor of $\sim$1.4. The reason for this discrepancy is not known at this time; the most likely explanation, however, is that the crystal orientation was different when the two sets of data were taken.

Fig. 10 is a plot of log (T_2, T_1, and $T_{1\rho}$) vs. 1/T for potassium-doped β-PbF_2. Both sets of T_2 data are given. The two data sets yield the same slope, within experimental error. These slopes give activation energies of 0.18 ± 0.01 eV for $T_2(A)$ and 0.17 ± 0.01 eV for $T_2(B)$. The $T_{1\rho}$ curve has a minimum at T = -20°C. The activation energy for $T_{1\rho}$ at temperatures below the minimum is 0.34 ± 0.02 eV. No T_1 minimum was observed in the temperature range of this experiment. An activation energy for T_1 is not well defined because of the gentle curve in the T_1 data. However, the three points taken at highest temperature appear to be collinear, and a line through these points gives an activation energy of 0.17 ± 0.01 eV.

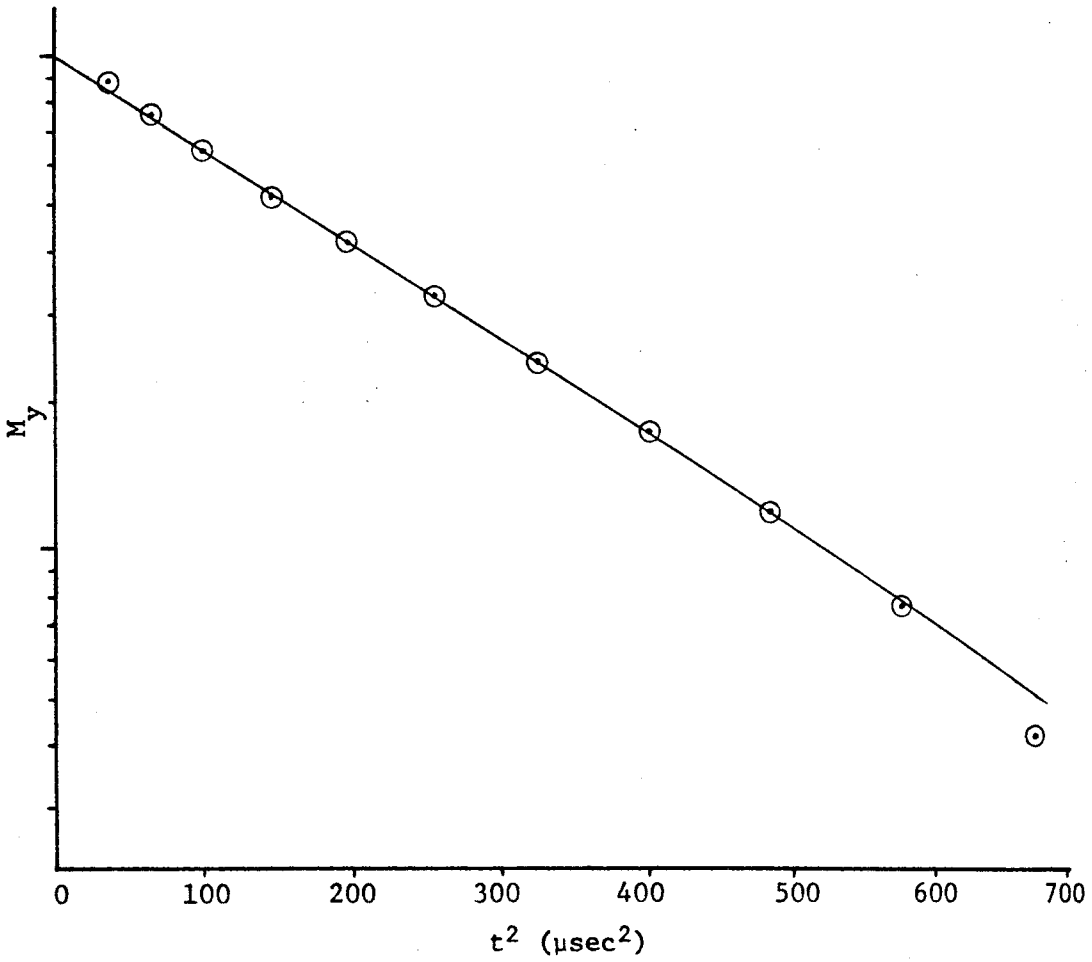

Fig. 5. Log of M_y vs. t^2 taken from fid data points at T = -69°C. The linearity of the plot demonstrates the Gaussian lineshape in this, the rigid lattice, temperature region.

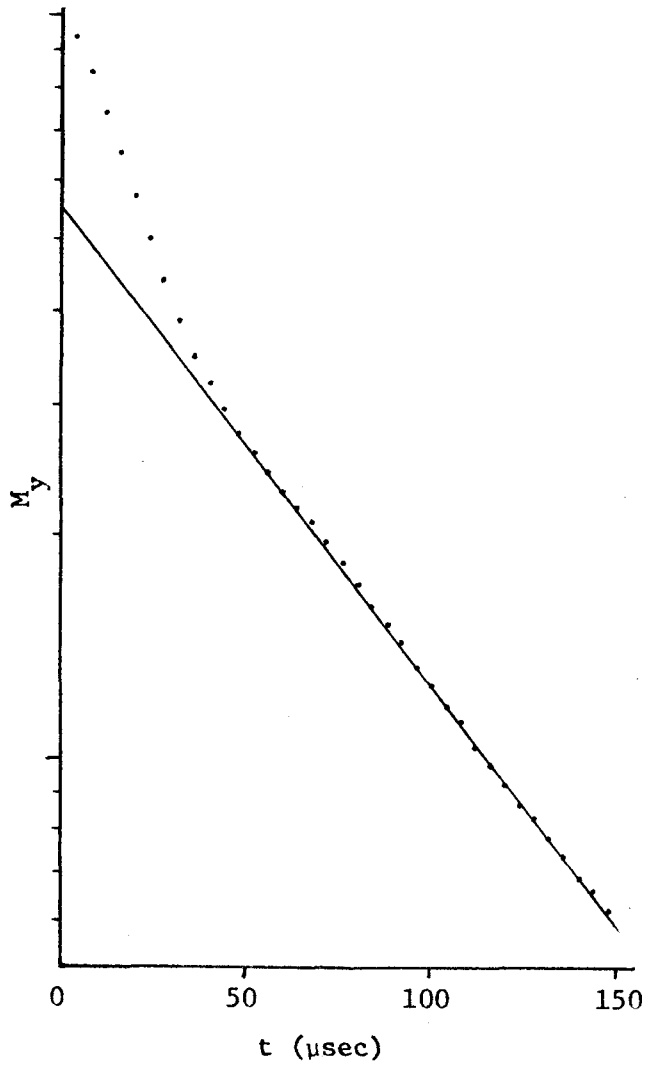

Fig. 6. Two-component fid taken at T = -40°C. Narrow component constitutes ∿55% of total signal. T_2 was taken as the slope of the line.

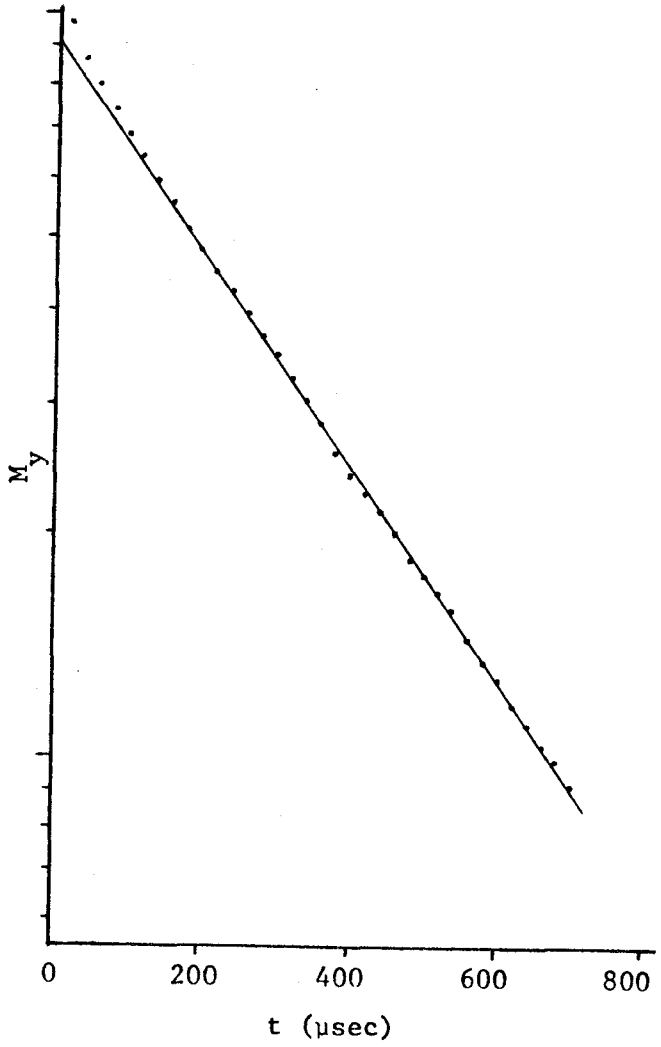

Fig. 7. Two-component fid taken at T = 9°C. Narrow component constitutes ∿93% of total signal. T_2 was taken as the slope of the line.

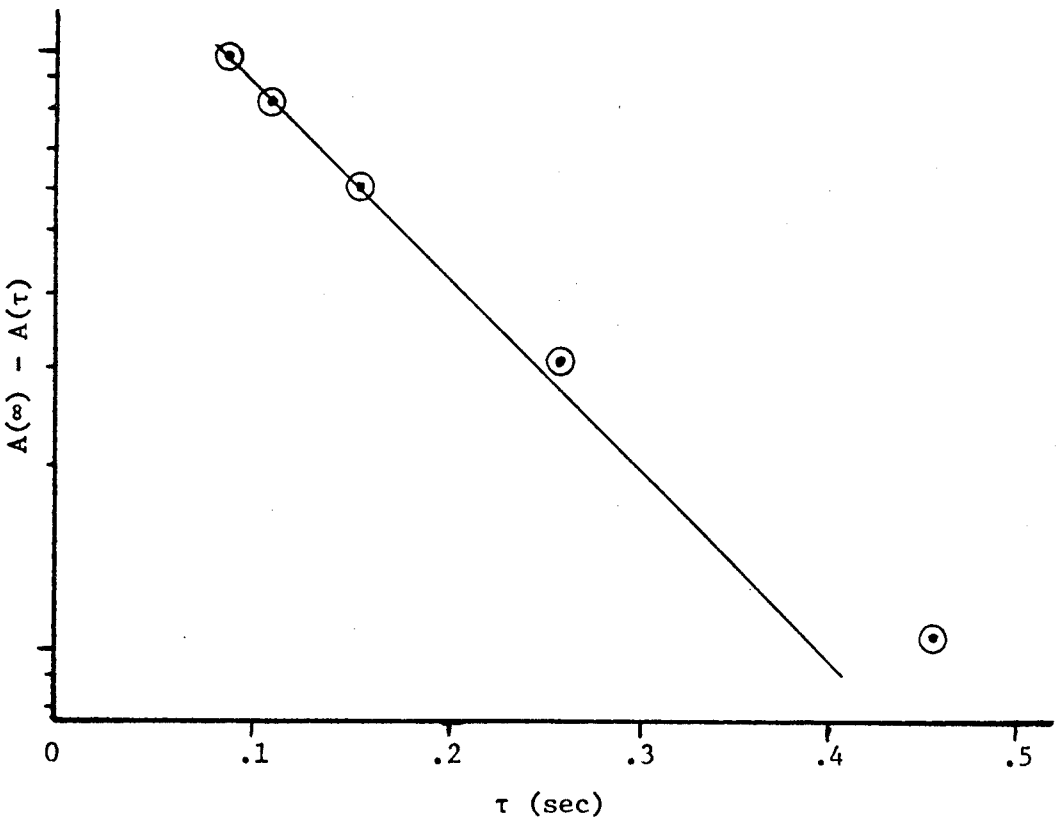

Fig. 8. T_1 decay taken at T = 6°C. T_1 was taken as the slope of the line shown above.

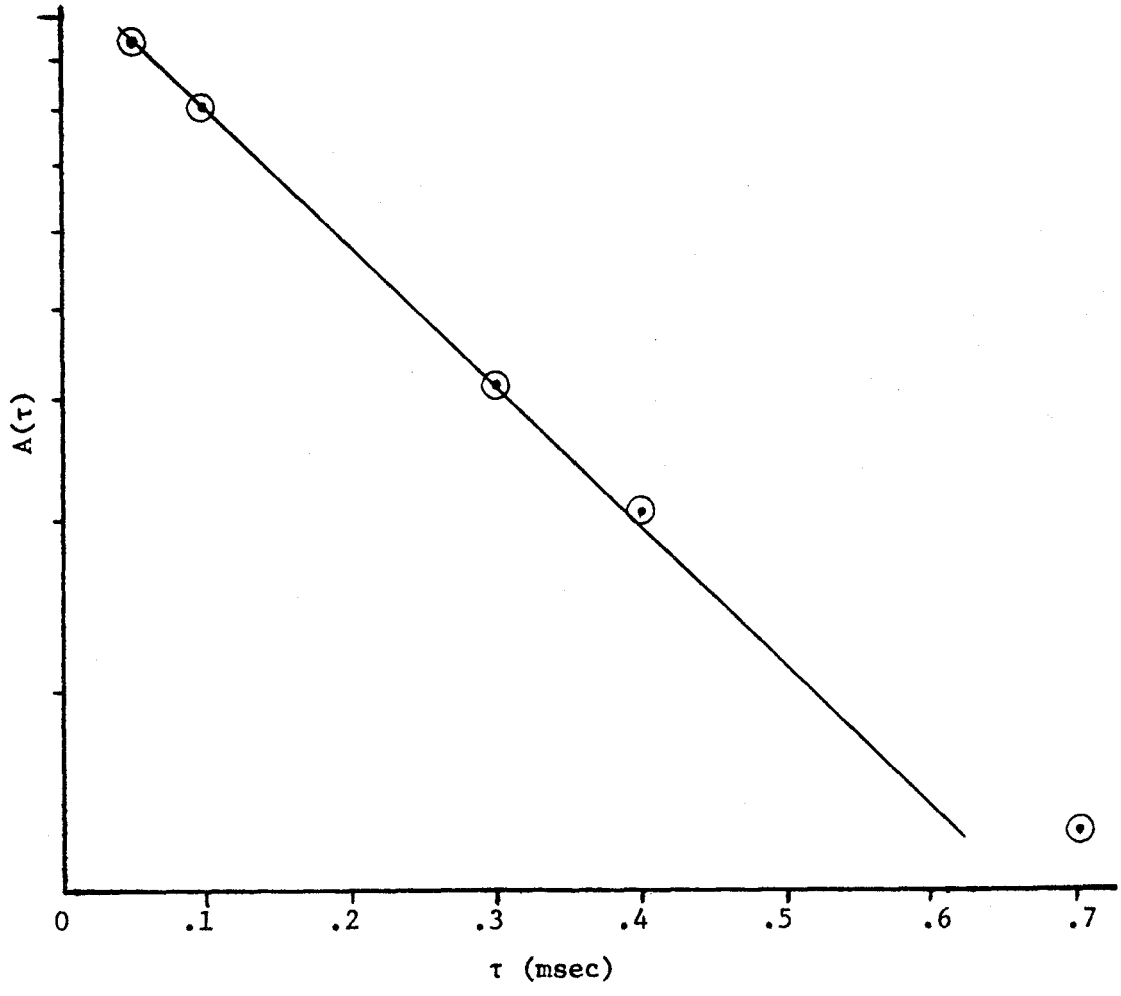

Fig. 9. $T_{1\rho}$ decay taken at T = -27°C. $T_{1\rho}$ was taken as the slope of the line shown above.

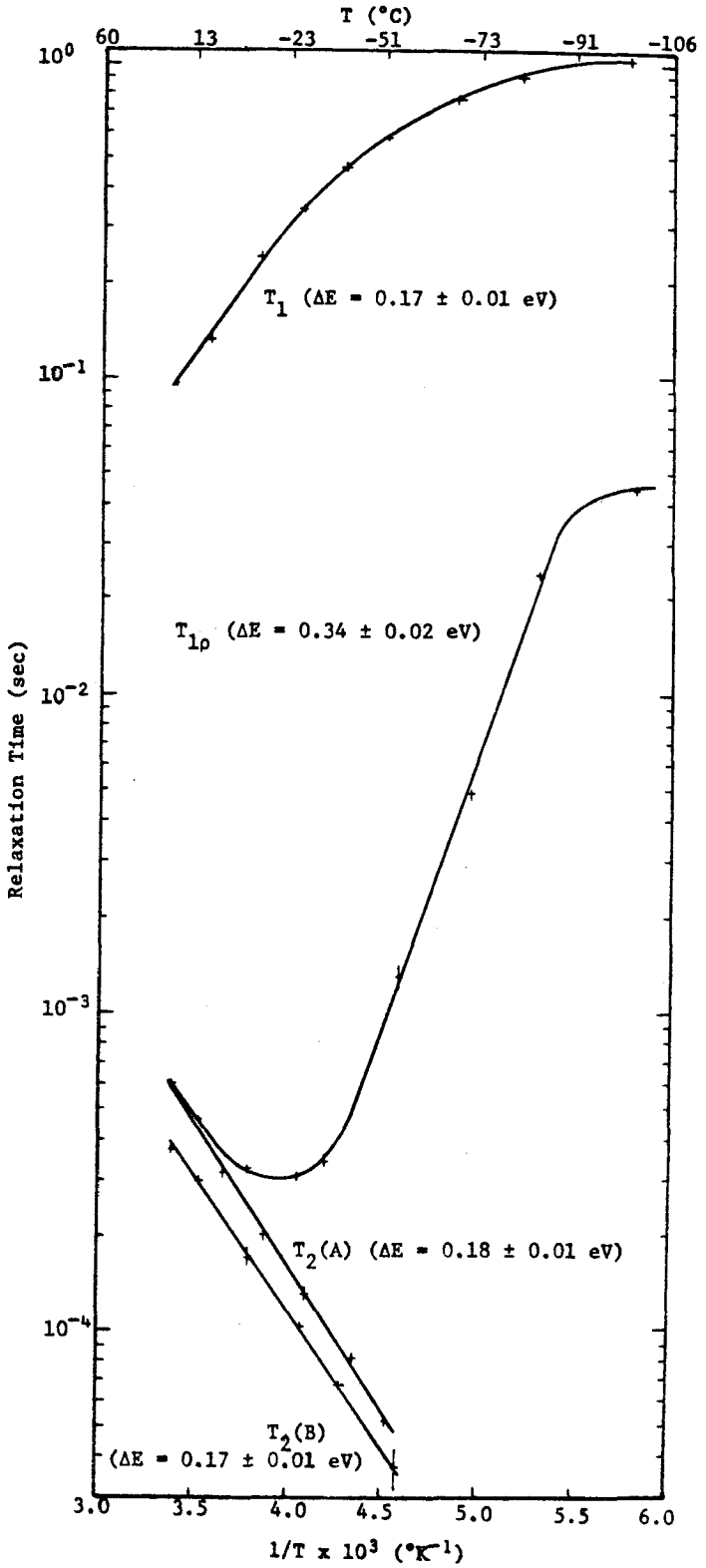

Fig. 10. Log of relaxation times vs. 1/T. Vertical error bars represent an estimate of precision for each T_1, $T_{1\rho}$, or T_2 value. Horizontal bars are uncertainty in measuring T.

Discussion

From the relationship $2\omega_1\tau_c = 1$ at the $T_{1\rho}$ minimum, a value of $\tau_c = 2.9$ μsec at T = -20°C is obtained. This compares with $\tau_c \approx 16$ μsec at -20°C which is estimated from the data of Hwang et al.[24] for a sodium-doped crystal with a higher dopant concentration. This comparison suggests that potassium-doping is more effective than sodium-doping in activating fluorine motion.

An estimate of the fluorine diffusion coefficient can be made from the relation $D = d^2/6\tau_c$ where d is the jump distance of a fluorine atom. Letting d = 2.96 Å (the fluorine-fluorine nearest neighbor distance) and $\tau_c = 2.9$ μsec gives $D = 5.0 \times 10^{-11}$ cm^2/sec at -20°C. This is consistent with the value obtained by extrapolating the conductivity data of Liang and Joshi[6] to the same temperature. A quantitative comparison is not meaningful since the samples used in the two experiments contained different concentrations of KF dopant.

An estimate was made of the expected contribution of fluoride ion motion to the relaxation rates $1/T_1$, $1/T_2$, and $1/T_{1\rho}$. The calculated values of T_2 and $T_{1\rho}$ at -20°C are in good agreement with observed values at that temperature. However, the experimentally determined T_1 is about two orders of magnitude smaller than the calculated value. This same phenomenon was reported by Hwang et al.[24] who inferred that T_1 must be controlled by a mechanism other than fluorine motion. They suggested that electronic carriers might be responsible for T_1 in sodium-doped PbF_2. That mechanism may dominate T_1 in the present case as well, although there is no direct evidence that that is the case.

If T_2 and $T_{1\rho}$ are both controlled by simple fluorine motion,

the activation energies of these two processes should be equal. The energies of activation for the two sets of T_2 data agree with the value of $\Delta H = 0.18$ eV reported by Liang and Joshi[6] for their potassium-doped samples. However, the activation energy obtained for $T_{1\rho}$ is twice that for T_2. We are presently unable to account for this difference.

The two-component relaxation curves which are observed in this experiment have not been reported in previous NMR studies of lead fluoride. The presence of more than one component reduces the accuracy of the relaxation data and complicates their interpretation. It is not known whether this behavior is caused by sample inhomogeneity or by some fundamental aspect of the diffusion process.

Conclusion

The results which have been obtained in this experiment are both interesting and perplexing. The NMR data for this potassium-doped β-PbF_2 crystal demonstrate anion mobility comparable to or greater than that reported for other β-PbF_2 samples. However, the quality of the crystal was less than expected, and this resulted in unforeseen complications. Further work in this area would be warranted if a crystal of better quality can be obtained.

References

[1] R.W.G. Wyckoff, Crystal Structures, 2nd edition, vol. 1 (Wiley-Interscience, New York, 1963) p. 240.

[2] Ya. Sauka, J. General Chem. USSR 19, 1453 (1949); from Chem. Absts. 44, 896i (1950).

[3] J.H. Kennedy, R. Miles, and J. Hunter, J. Electrochem. Soc. 120, 1441 (1973).

[4] D.A. Jones, Proc. Phys. Soc. London, Sect. A 68, 165 (1955).

[5] C. Tubandt, Z. Anorg. Chem. 115, 105 (1921).

[6] C.C. Liang and A.V. Joshi, J. Electrochem. Soc. 122, 466 (1975).

[7] R. Benz, Z. Phys. Chem. Neue Folge 95, 25 (1975).

[8] J. Schoonman, G.A. Korteweg, and R.W. Bonne, Solid State Commun. 16, 9 (1975).

[9] A.V. Joshi and C.C. Liang, J. Electrochem. Soc. 124, 1253 (1977).

[10] J. Schoonman, G.J. Dirksen, and G. Blasse, J. Solid State Chem. 7, 245 (1973).

[11] J.C. Gianduzzo, J. Pistre, and J. Salardenne, Electrocomponent Sci. Technol. 2, 55 (1975).

[12] J.M. Reau, J. Claverie, G. Campet, C. Deportes, D. Ravaine, J.L. Souquet, and A. Hammou, C.R. Acad. Sci., Ser. C 280, 325 (1975); from Chem. Absts. 83, 19959e (1975).

[13] V.A. Arkhangel'skaya, V.G. Erofeichev, and M.N. Kiseleva, Sov. Phys.-Solid State 14, 2953 (1973).

[14] J. Schoonman, L.B. Ebert, C-H. Hsieh, and R.A. Huggins, J. Appl. Phys. 46, 2873 (1975).

[15] J.H. Kennedy and R.C. Miles, J. Electrochem. Soc. 123, 47 (1976).

[16] R.W. Bonne and J. Schoonman, Solid State Commun. 18, 1005 (1976).

[17] I.D. Raistrick, C. Ho, Y.W. Hu, and R.A. Huggins, J. Electroanal. Chem. 77, 319 (1977).

[18] R.W. Bonne and J. Schoonman, J. Electrochem. Soc. 124, 28 (1977).

[19] C.E. Derrington and M. O'Keeffe, Nature (London), Phys. Sci. 246, 44 (1973).

[20]C.C. Liang and A.V. Joshi, J. Electrochem. Soc. 122, 1642 (1975).

[21]M. Mahajan and B.D. Rao, Chem. Phys. Lett. 10, 29 (1971).

[22]P.P. Mahendroo, N.S.K. Menon, and J.L. Marchant, Magn. Reson. Relat. Phenom., Proc. Congr. AMPERE, 18th 1, 237 (1974).

[23]T.Y. Hwang, M. Engelsberg, and I.J. Lowe, Chem. Phys. Lett. 30, 303 (1975).

[24]T.Y. Hwang, I.J. Lowe, K.F. Lau, and R.W. Vaughan, J. Chem. Phys. 65, 912 (1976).

[25]J.B. Boyce, J.C. Mikkelsen, M. O'Keeffe, Solid State Commun. 21, 955 (1977).

[26]R.D. Hogg, S.P. Vernon, and V. Jaccarino, Phys. Rev. Lett. 39, 481 (1977).

[27]T.C. Farrar and E.D. Becker, Pulse and Fourier Transform NMR (Academic Press, New York, 1971).

APPENDIX: PULSED-NMR LOCK SYSTEM

Before this thesis project was undertaken, a new pulsed-NMR lock system was constructed to replace the cw system which was previously in use on our 56.4 MHz spectrometer. The new system contains a crystal oscillator which produces an rf signal at a desired frequency. This signal is gated to produce rf pulses which are amplified and sent through a quadrature hybrid to the sample probe. The probe transmits the rf pulses to the sample and receives the NMR signal in return. This signal is sent back through the quadrature hybrid to a "receiver" where it is amplified. Since the probe receives and transmits signals, the quadrature hybrid is used to isolate the receiver from the rf pulses. The signal from the receiver is phase detected to produce a slightly off-resonant free induction decay (fid) signal. A sample-and-hold device samples a small part of the fid at a zero-crossing and an integrator accumulates these samplings over time. The integrator thus produces a dc signal whose level will be zero if the system is properly locked. If the integrated signal is non-zero a flux stabilizer adjusts the magnet current until proper locking is achieved.

This system is schematized in Fig. 11. I was responsible for building the rf part of the system, the part lying above the dashed line in Fig. 11. The digital part of the system was constructed by the Chemical Engineering Electronics Shop.

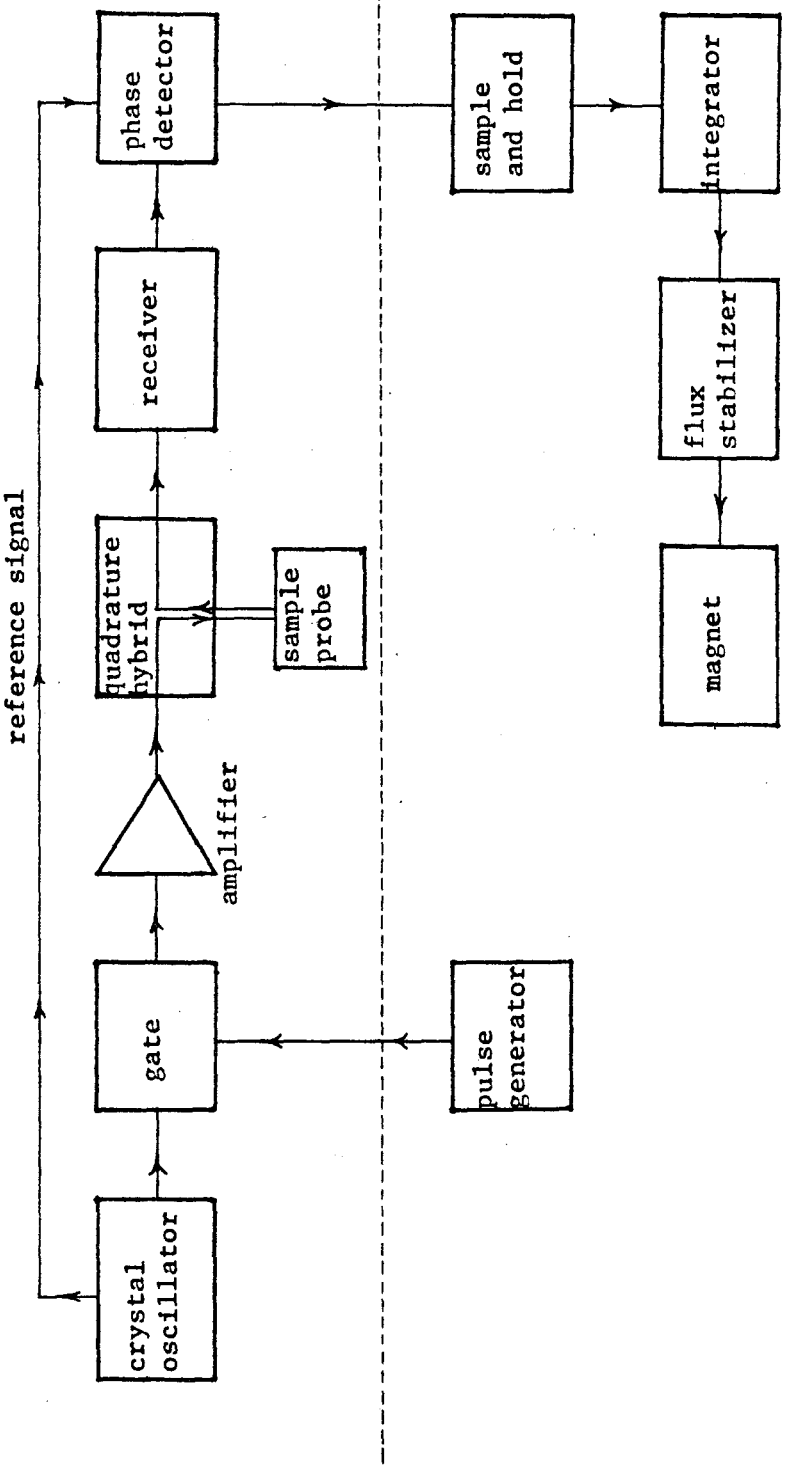

Fig. 11. Schematic of pulsed-NMR lock system.